2 cells were cultured in the absence (None) or presence of IC50 values of 4-OHCY or chlorambucil (CB), harvested at the indicated time points, and stained with propidium iodide in preparation for cell cycle analysis. Columns indicate the quantification of cells in each phase of the cell cycle obtained with the ModFitLT 2.0 program. The means ± S.D. (bars) of three independent experiments are shown. *P*-values were calculated by one-way ANOVA with the Student-Newman-Keuls multiple comparisons test. Asterisks denote $p<0.05$ against the untreated control.
doi:10.1371/journal.pone.0090675.g001

leukemia (CLL) [8] and rituximab-resistant low-grade lymphomas [9], and in combination with rituximab for patients with follicular lymphoma and mantle cell lymphoma [10,11]. The spectrum of the clinical application of bendamustine is further expanding to diffuse large B-cell lymphoma (DLBCL) [12], aggressive lymphomas [13,14], multiple myeloma [15,16], T-cell lymphomas [17] and solid tumors [18,19]. Although bendamustine monotherapy and the combination with rituximab appear to be successful for CLL and untreated indolent lymphomas [8,11], combined chemotherapy with other therapeutic agents is required for the treatment of relapsed cases and refractory malignancies such as multiple myeloma and aggressive lymphomas.

Combined chemotherapy remains the primary approach for patients with hematological malignancies. The anti-cancer agents used for combination are generally selected on the basis of single-agent activity, non-overlapping toxicity, and the lack of cross-resistance and antagonistic interaction. In addition, mechanistic insight is important for the establishment of effective and safe regimens. In the case of bendamustine, its unique mechanisms of action may influence the selection of drugs to be combined. Previous preclinical studies have demonstrated the combined effects of bendamustine with cytosine arabinoside, gemcitabine, fludarabine, cladribine, mitoxantrone, doxorubicin and entinostat [5,6,20–24]. Some of the combinations have been clinically translated with anticipated success [25–28], but theoretical basis of their effects requires independent validation. To establish more effective and safer regimens, we systematically screened for suitable drugs to be combined with bendamustine for intractable lymphoid malignancies and investigated the mechanisms underlying favorable combinations in the present study. Among lymphoid malignancies, we focused on mantle cell lymphoma, DLBCL, Burkitt lymphoma and multiple myeloma, because of their relative resistance to bendamustine monotherapy in clinical settings [12–16]. We found that bendamustine made favorable combinations with alkylating agents and pyrimidine analogues in these tumors at least partly due to its purine analog-like properties. This finding may provide important information for the establishment of effective bendamustine-based regimens.

Materials and Methods

Drugs

Bendamustine was provided by SymBio Pharmaceuticals Ltd. (Tokyo, Japan). Other anti-cancer agents used and their sources are 4-hydroperoxy-cyclophosphamide (4-OHCY; an active metabolite of cyclophosphamide) (Shionogi, Osaka, Japan), chlorambucil (LKT Laboratories, St. Paul, MN, USA), melphalan (Wako Biochemicals, Osaka, Japan), cytosine arabinoside (Ara-C) (Nihon Shinyaku, Kyoto, Japan), gemcitabine (Eli Lilly, Kobe, Japan), decitabine (Sigma-Aldrich, St. Louis, MO, USA), 9-ß-D-arabinosyl-2-fluoroadenine (F-Ara-A; an active metabolite of fludarabine) (Sigma-Aldrich), doxorubicin (Meiji, Tokyo, Japan), mitoxantrone (Lederle Japan, Tokyo, Japan), etoposide (Nihon Kayaku, Tokyo, Japan), methotrexate (Lederle Japan), vincristine (Shionogi) and bortezomib (LC Laboratories, Wobum, MA, USA). Dilazep (N,N'-bis-(E)-[5-(3,4,5-trimethoxy-baenzoate)-4-pentenyl] homopiperazine) was provided by Kowa Pharmaceuticals (Tokyo, Japan). S-(4-nitrobenzyl)-6-thioinsine (NBTI) was purchased from Sigma-Aldrich.

Cell Lines

We used two multiple myeloma (U266 and RPMI 8226), two Burkitt lymphoma (BJAB and Namalwa), four mantle cell lymphoma (HBL-2, SMCH-16, Granta519 and NCEB-1), two diffuse large B-cell lymphoma (TK and B104), two T-cell acute lymphoblastic leukemia (Jurkat and KOPT-5) and three acute myeloid leukemia (HL-60, K562 and THP-1) cell lines for drug sensitivity screening. These were purchased from the Health Science Research Resources Bank (Osaka, Japan) except for mantle cell lymphoma cell lines [29,30].

Cell Proliferation Assay

Cells were harvested at the logarithmic phase and resuspended at $1–5\times10^5$ cells/ml in RPMI1640 medium containing 10% fetal bovine serum. After overnight culture in a humidified atmosphere of 95% air/5% CO2 at 37°C, drug solutions were added and cells were further incubated for given culture periods. Viable cell numbers were estimated by the reduction of 3-(4,5-dimethylthiazol-2-yl)-2,5-diphenyltetrazolium bromide (MTT) using a Cell Counting Kit (Wako Biochemicals). Absorbance at 450-nm (A450) was determined with a microplate reader and expressed as a ratio of the value of corresponding untreated cells.

Drug Combination Study

To analyze cytotoxic interactions, we cultured cells in the presence of 0, 20, 40, 60, 80 and 100% of IC50 and IC80 doses of bendamustine and another drug simultaneously for 96 hours. The combined effects were evaluated by the isobologram method of Steel and Peckham as described previously [31,32]. In brief, three isoeffect curves are constructed based on the dose-response curve of bendamustine and another drug. If two agents act additively by independent mechanisms, their combined data points will lie near the line of hetero-addition. If agents act additively by similar mechanisms, their combined data points will lie near the lines of iso-addition (Figure S1). Because the difference in IC levels did not affect the conclusions, we present only the results of the IC80 level. We statistically analyzed overall effects of drug combination using Wilcoxon signed-rank test. If the observed values are significantly ($P<0.05$) smaller than the predicted minimum values, the combination is regarded as synergistic. If P values are greater than 0.05, the combination is regarded as additive/synergistic. If the observed data fall between the predicted minimum and maximum values, the combination is regarded as additive.

Cell Cycle Analysis

The cell cycle profile was obtained by staining DNA with Vindelov's solution (0.04 mg/ml propidium iodide in 5 mM Tris-HCl, 5 mM NaCl and 0.005% Nonidet P-40) in preparation for flow cytometry with the FACScan/CellFIT system (Becton-Dickinson, San Jose, CA). The size of the sub-G1, G0/G1 and S+G2/M fractions was calculated as a percentage by analyzing DNA histograms with the ModFitLT 2.0 program (Becton-Dickinson).

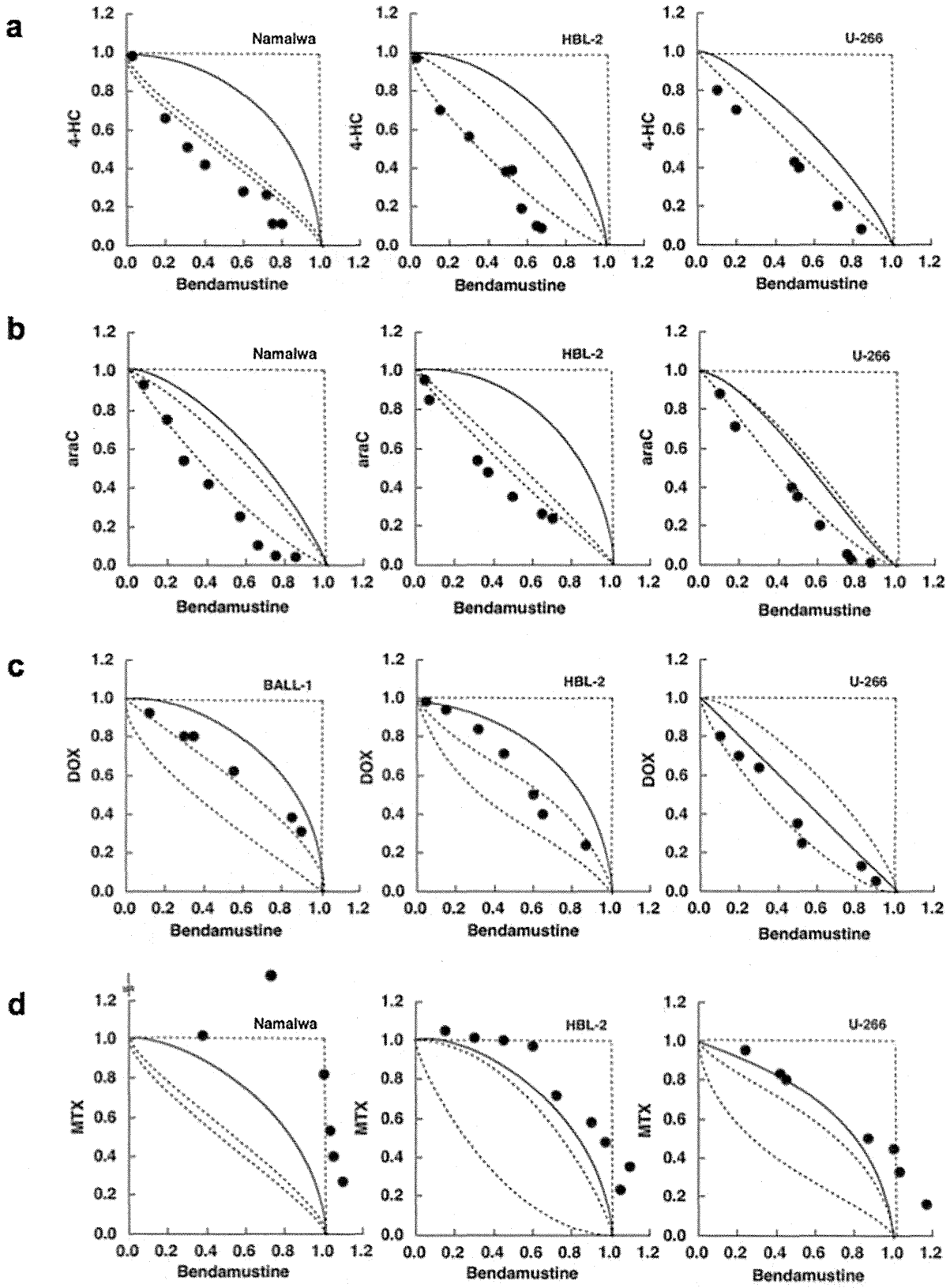

Figure 2. The selection of suitable drugs to be combined with bendamustine using isobologram. Cells were cultured with various concentrations of bendamustine in combination with (A) 4-hydroperoxy-cyclophosphamide (4-HC), (B) cytosine arabinoside (araC), (C) doxorubicin (DOX) and (D) methotrexate (MTX) for 4 days (Namalwa and HBL-2) or 7 days (U266). Isobolograms were generated from dose-response curves of each combination as described previously [31,32]. The results of data quantification and statistical analysis are shown in Table 1.
doi:10.1371/journal.pone.0090675.g002

Table 1. Quantitative analysis of the combination of bendamustine and other drugs in lymphoid malignancies.

Combined drugs	Cell lines	Data points	Observed data*	Predicted mini.**	Predicted max.***	Effects#
4-OHCY	HBL-2	8	0.44	0.47	0.81	additive/synergistic
	B104	4	0.47	0.58	0.82	synergistic
	Namalwa	5	0.38	0.51	0.79	synergistic
	U266	6	0,55	0.62	0.75	synergistic
Ara-C	HBL-2	7	0.45	0.49	0.83	synergistic
	B104	5	0.44	0.55	0.79	synergistic
	Namalwa	5	0.51	0.63	0.80	synergistic
	U266	8	0.68	0.74	0.86	synergistic
Gemcitabine	HBL-2	7	0.37	0.45	0.92	synergistic
	B104	4	0.40	0.51	0.93	synergistic
	Namalwa	6	0.39	0.45	0.78	synergistic
	U266	7	0.35	0.45	0.82	synergistic
Decitabine	HBL-2	5	0.47	0.61	0.89	synergistic
	B104	4	0.41	0.52	0.74	synergistic
	Namalwa	7	0.45	0.48	0.84	additive/synergistic
	U266	7	0.39	0.57	0.78	synergistic
F-Ara-A	HBL-2	8	0.42	0.36	0.90	additive
	B104	4	0.48	0.41	0.83	additive
	Namalwa	4	0.59	0.55	0.77	additive
	U266	7	0.53	0.33	0.85	additive
Doxorubicin	HBL-2	6	0.63	0.42	0.86	additive
	B104	4	0.59	0.48	0.81	additive
	Namalwa	5	0.68	0.35	0.78	additive
	U266	7	0.62	0.54	0.84	additive
Mitoxantrone	HBL-2	7	0.55	0.52	0.86	additive
	B104	4	0.55	0.43	0.66	additive
	Namalwa	5	0.61	0.38	0.72	additive
	U266	7	0.52	0.51	0.57	additive
Etoposide	HBL-2	9	0.61	0.42	0.87	additive
	B104	4	0.59	0.48	0.84	additive
	Namalwa	4	0.65	0.57	0.80	additive
	U266	9	0.65	0.53	0.95	additive
Methotrexate	HBL-2	9	0.93	0.22	0.80	antagonistic
	B104	4	0.98	0.44	0.75	antagonistic
	Namalwa	5	1.02	0.45	0.68	antagonistic
	U266	7	0.71	0.36	0.68	antagonistic
Vincristine	HBL-2	7	0.60	0.40	0.74	additive
	B104	4	0.55	0.42	0.71	additive
	Namalwa	5	0.59	0.46	0.77	additive
	U266	6	0.57	0.40	0.72	additive
Bortezomib	HBL-2	11	0.44	0.58	0.81	additive/synergistic
	B104	4	0.53	0.59	0.88	additive/synergistic
	Namalwa	5	0.62	0.53	0.79	synergistic
	U266	6	0.87	0.63	0.99	additive

*Mean values of observed data (S.D. not shown).
**Mean values of the predicted minimum values for an additive effect (S.D. not shown).
***Mean values of the predicted maximum values for an additive effect (S.D. not shown).
#Overall effect of drug combination (see Materials and Methods for the method of evaluation).
doi:10.1371/journal.pone.0090675.t001

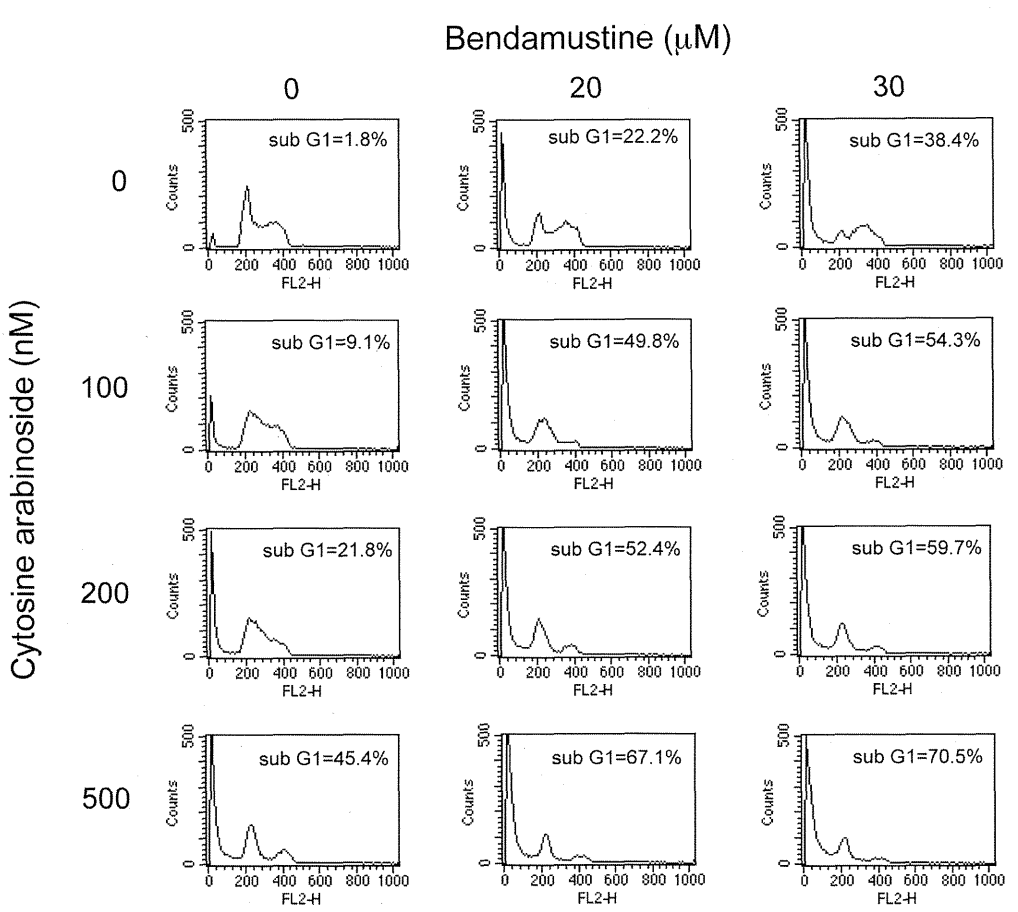
a
Bendamustine (μM)
0
20
30
Cytosine arabinoside (nM)
0
100
200
500
sub G1=1.8%
sub G1=22.2%
sub G1=38.4%
sub G1=9.1%
sub G1=49.8%
sub G1=54.3%
sub G1=21.8%
sub G1=52.4%
sub G1=59.7%
sub G1=45.4%
sub G1=67.1%
sub G1=70.5%
Counts
FL2-H

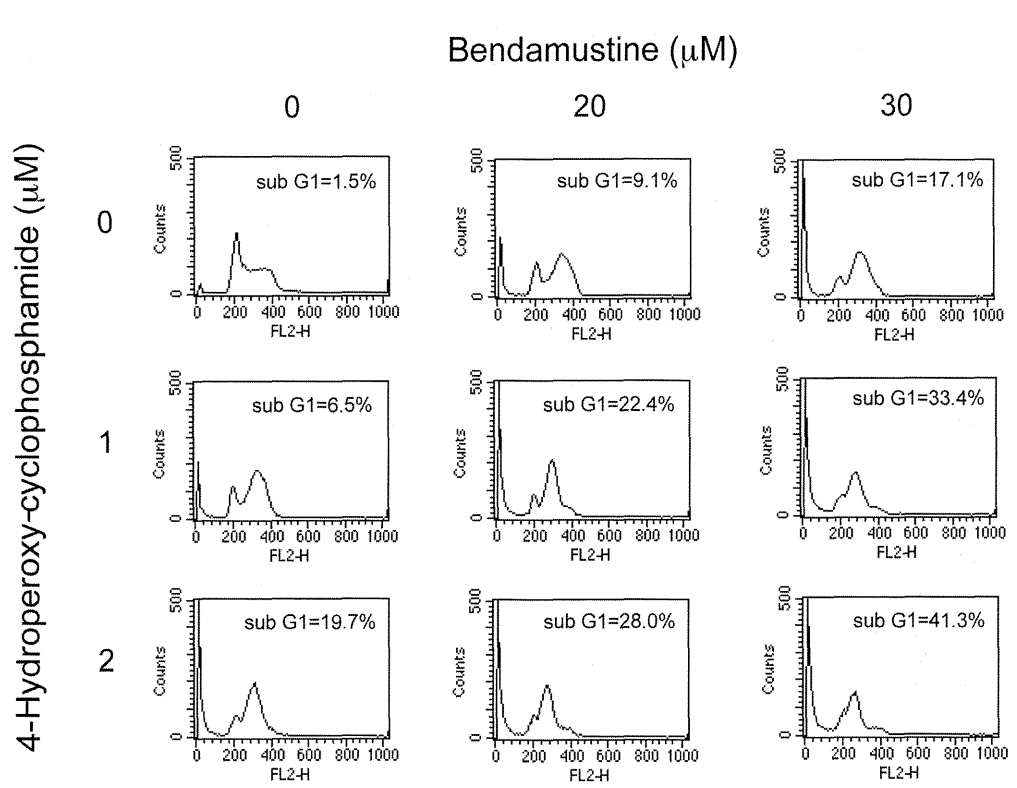
b
Bendamustine (μM)
0
20
30
4-Hydroperoxy-cyclophosphamide (μM)
0
1
2
sub G1=1.5%
sub G1=9.1%
sub G1=17.1%
sub G1=6.5%
sub G1=22.4%
sub G1=33.4%
sub G1=19.7%
sub G1=28.0%
sub G1=41.3%
Counts
FL2-H

Figure 3. Cell cycle effects of the combination of bendamustine with 4-OHCY or cytosine arabinoside. (A) HBL-2 cells were cultured with bendamustine alone, cytosine arabinoside alone or their combination for 48 hours. (B) HBL-2 cells were cultured with bendamustine alone, 4-OHCY alone or their combination for 48 hours. Cell cycle profiles were obtained by flow cytometry as described in Materials and Methods. The size of the sub-G1 fraction was calculated by analyzing DNA histograms with the ModFitLT 2.0 program. The data shown are representative of multiple independent experiments with various concentrations of the drugs.
doi:10.1371/journal.pone.0090675.g003

Cell Culture

We examined the effect of ENT1 inhibitors on anti-cancer drugs according to previous reports [33]. In brief, HBL-2 and Namalwa cells were cultured in the absence or presence of IC50 doses of cytosine arabinoside, F-Ara-A, bendamustine and 4-OHCY (10, 2.5, 25 and 2 μM, respectively) with various concentrations of either dilazep or NBTI for 72 hours. Relative cytotoxic effects were calculated according to the following formula: 1- (A450 in the presence of both drugs and inhibitors/A450 in the presence of inhibitors alone)/1- (A450 in the presence of drugs alone/A450 in the presence of inhibitors alone) × 100.

We compared the combined effects of bendamustine and cytosine arabinoside between simultaneous and sequential additions. In the former, HBL-2 cells were cultured in the presence of various concentrations of the two drugs for 48 hours. In case of sequential additions, HBL-2 cells were cultured with various concentrations of either cytosine arabinoside or bendamustine for 48 hours, washed with phosphate-buffered saline, resuspended in the complete medium containing various concentrations of either bendamustine or cytosine arabinoside, and cultured for additional 48 hours. Isobolograms with then generated from dose-response curves obtained under each condition.

Immunoblotting

HBL-2 and Namalwa cells were cultured in the absence or presence of IC50 doses of each drug. Whole cell lysates were isolated at given time points and subjected to immunoblot analysis using specific antibodies against phosphorylated Chk1 at Ser-296, phosphorylated Chk2 at Thr-68 (Cell Signaling Technology, Beverly, MA), ENT1 (F-12), ENT2 (H-46) and GAPDH (FL-335) (Santa Cruz Biotechnology, Santa Cruz, CA) [34].

Real-time Quantitative RT-PCR

HBL-2 and Namalwa cells were cultured in the absence or presence of IC50 doses of 4-OHCY, bendamustine or F-Ara-A (2, 25 and 2.5 μM, respectively). Total cellular RNA was isolated after 48 hours using the RNeasy Kit (QIAGEN, Valencia, CA) and reverse-transcribed into cDNA using ReverTra Ace and oligo (dT) primers (TOYOBO, Tokyo, Japan). We performed real-time quantitative RT-PCR using the TaqMan Gene Expression Assay System (Hs01085704 for *SLC29A1/ENT1* and Hs01922876 for *GAPDH*) with TaqMan Fast Universal PCR Master Mix (Applied Biosystems, Warrington, UK) as described previously [35]. The data were quantified with the $2^{-\Delta\Delta Ct}$ method using simultaneously amplified *GAPDH* as a reference.

Measurement of Ara-C and F-Ara-A Uptake

We measured cellular uptake of Ara-C and F-Ara-A using [5-^{3}H]Ara-C and [8-^{3}H]F-Ara-A (Moravek Biochemicals, Brea, CA, USA) as described previously [36]. Briefly, HBL-2 cells (1×10^6 cells/ml) were incubated with 10 μM F-Ara-A or bendamustine for 3 h at 37°C, followed by washing into fresh media and subsequent incubation with either [5-^{3}H]Ara-C or [8-^{3}H]F-Ara-A at 10 μM (30 Ci/mmol) for 6 h at 37°C. The samples were then centrifuged to collect the cell pellets (400×*g*, 10 min, 4°C). The acid-soluble fraction, the nucleotide pool, was extracted by adding perchloric acid, followed by neutralization with KOH, and subjected to scintillation counting for radioactivity detection.

Determination of Intracellular Ara-CTP

HBL-2 cells (1×10^6 cells/ml, 10 ml) were incubated with or without 10 μM (final concentration) F-Ara-A or 10 μM (final concentration) bendamustine for 3 h at 37°C, followed by washing into fresh media and subsequent incubation with 10 μM (final concentration) Ara-C for 6 h at 37°C. The acid-soluble fraction was prepared as described above. The intracellular active metabolite of Ara-C, Ara-CTP, was determined as described previously [37]. Briefly, the samples were subjected to isocratic high-performance liquid chromatography (HPLC) using a TSK gel DEAE-2 SW column (length, 250 mm; internal diameter, 4.6 mm) (Tosoh, Tokyo, Japan) and 0.06 M Na2HPO4 (pH 6.9) −20% acetonitrile buffer (a constant flow rate of 0.7 ml/min and at ambient temperature). The Ara-CTP peak was identified by its retention time and quantitated from its peak area at an absorbance of 269 nm.

Results

Bendamustine Induces Apoptosis Faster than other Alkylating Agents but does not Exert Sufficient Cytotoxicity against all Tumors

Bendamustine has a unique anti-tumor spectrum according to the *In Vitro* Cell Line Screening Project (IVCLSP) and National Cancer Institute (NCI) COMPARE analyses [4]. In this study, we first attempted to confirm the unique pattern of cytotoxicity in hematologic malignancies. As shown in Figure 1A, bendamustine displayed considerable cytotoxicity against cell lines derived from mantle cell lymphoma (HBL-2 and SMCH16), Burkitt lymphoma (BJAB and Namalwa) and T-cell acute lymphoblastic leukemia (Jurkat and KOPT-5), whereas the effects on acute myeloid leukemia and myeloma cell lines were relatively weak. In addition, the DLBCL cell lines, TK and B104, had intermediate sensitivity to bendamustine with IC50 values of 47.0±4.6 and 42.0±6.9 μM, respectively. It is of note that two of four mantle cell lymphoma cell lines (Granta519 and NCEB-1) were highly resistant to this drug.

To understand the nature of bendamustine-mediated growth inhibition, we analyzed the cell cycle pattern of bendamustine-treated HBL-2 and Namalwa cells. The IC50 value of bendamustine (25 μM) induced S-phase arrest at an early time point (12 hours), followed by a time-dependent increase in the size of sub-G1 fractions (Figure 1B). On the other hand, the IC50 values of 4-OHCY and chlorambucil neither induced cell cycle arrest nor increased the size of sub-G1 fractions within 24 hours (Figure 1C). As the sub-G1 fraction is caused by apoptosis-specific DNA fragmentation, these results indicate that bendamustine induces S-phase arrest and subsequent apoptosis faster than other alkylating agents. The induction of apoptosis was independently confirmed by annexin-V staining and caspase-3 activation (data not shown).

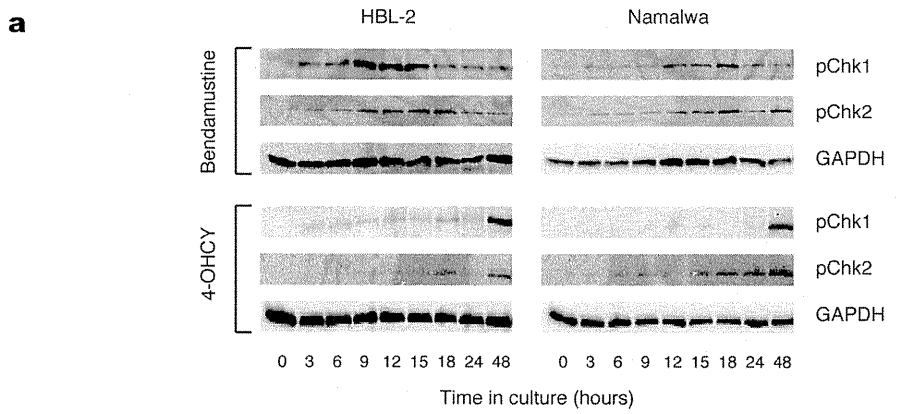
a
HBL-2
Namalwa
Bendamustine
4-OHCY
pChk1
pChk2
GAPDH
0 3 6 9 12 15 18 24 48
Time in culture (hours)

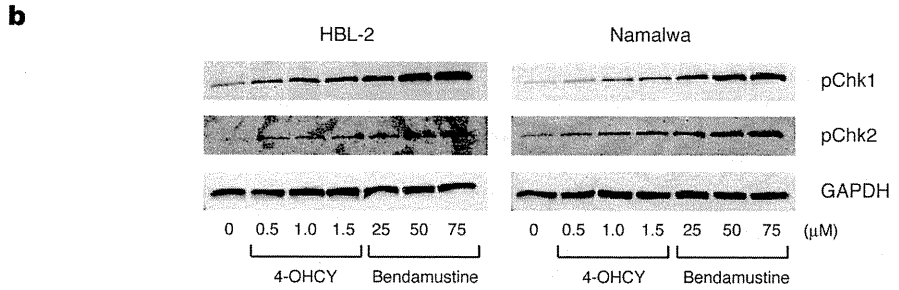
b
HBL-2
Namalwa
pChk1
pChk2
GAPDH
0 0.5 1.0 1.5 25 50 75 (μM)
4-OHCY
Bendamustine

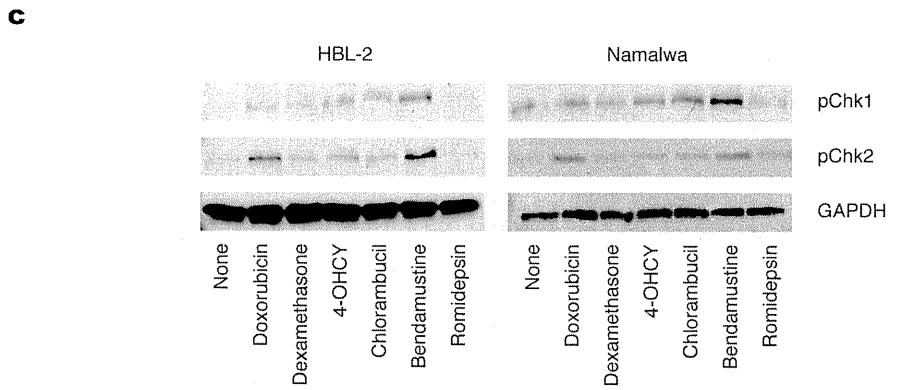
c
HBL-2
Namalwa
pChk1
pChk2
GAPDH
None
Doxorubicin
Dexamethasone
4-OHCY
Chlorambucil
Bendamustine
Romidepsin

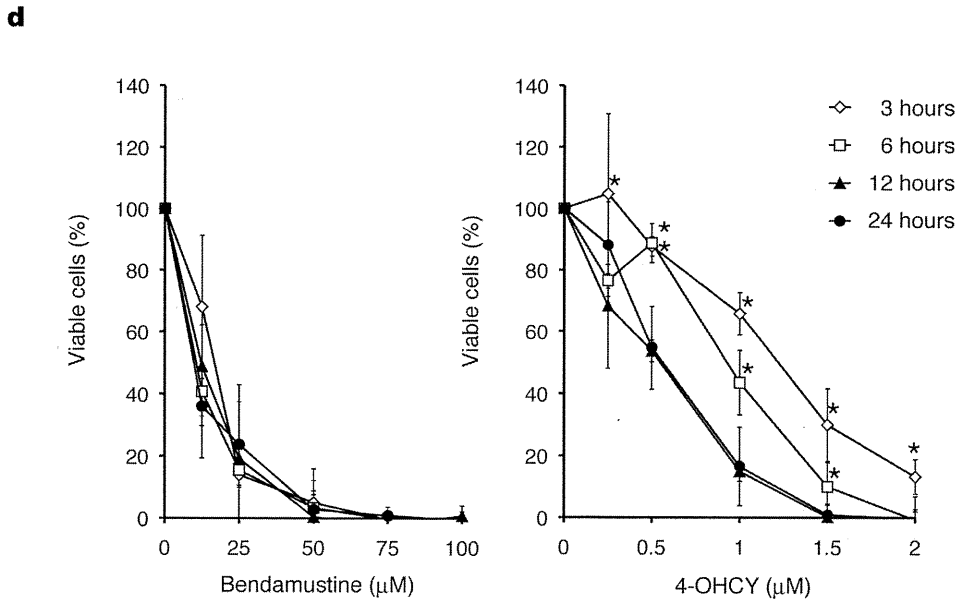
d
Viable cells (%)
Bendamustine (μM)
4-OHCY (μM)
3 hours
6 hours
12 hours
24 hours

Figure 4. Bendamustine elicits DNA damage response and subsequent apoptosis faster and with a shorter exposure time than other alkylating agents. (A) Time-course analysis of Chk1 and Chk2 phosphorylation in HBL-2 and Namalwa cells treated with IC50 values of bendamustine or 4-OHCY. (B) Dose-response analysis of Chk1 and Chk2 phosphorylation in HBL-2 and Namalwa cells treated with bendamustine or 4-OHCY for 12 hours. (C) Chk1 and Chk2 phosphorylation was detected in HBL-2 and Namalwa cells treated with IC50 values of the indicated drugs for 6 hours. The membranes were reprobed with anti-GAPDH antibody to serve as a loading control in each experiment. The data shown are representative of multiple independent experiments. (D) After treatment for the indicated periods (3–24 hours) with the indicated doses of bendamustine or 4-OHCY, HBL-2 cells were washed twice with fresh medium and cultured in complete medium without drugs. The cells were cultured for 72 hours in total and subjected to MTT assays. Panels show the dose-response curves of bendamustine- and 4-OHCY-treated cells. The means ± S.D. (bars) of three independent experiments are shown. *P*-values were calculated by one-way ANOVA with the Student-Newman-Keuls multiple comparisons test. Asterisks indicate $p<0.05$ against each value of 24 h exposure.
doi:10.1371/journal.pone.0090675.g004

The Selection of Suitable Drugs to be Combined with Bendamustine for Intractable Lymphoid Malignancies using Isobologram

Drug sensitivity screening revealed that the IC50 values of sensitive and resistant cell lines were 10–30 μM and 100–250 μM, respectively. This clearly indicates that combination with other anti-cancer agents is essential for the treatment of bendamustine-insensitive tumors, because bendamustine yielded a maximum serum concentration of approximately 25 μM after intravenous administration of the usual dose (120 mg/m^2) with a mean elimination half-life of 30–50 minutes [38,39]. We therefore analyzed cytotoxic interactions between bendamustine and 13 drugs that represent six different classes of cytotoxic agents in lymphoid malignancies relatively resistant to bendamustine monotherapy in clinical settings: mantle cell lymphoma (HBL-2), diffuse large B-cell lymphoma (B104), Burkitt lymphoma (Namalwa) and multiple myeloma (U266). To quantify cytotoxic interactions, we constructed isobolograms with three isoeffect curves (mode I and mode II lines) from dose-response curves of bendamustine and the combined drugs using data points at the IC80 and IC50 levels (Figure S1).

Figure 2A shows the representative isobolograms of the combination of bendamustine and 4-OHCY, in which all or most data points for the combination fell in the area of supra-additivity in all cell lines tested. The mean values of observed data were significantly smaller than those of the predicted minimum values for the additive effect in B104, Namalwa and U266, indicating a synergistic effect of the two drugs (Table 1). Similar results were obtained in combination with bendamustine and other alkylating agents such as chlorambucil and melphalan (data not shown). Figure 2B shows the isobolograms of the combination of bendamustine and cytosine arabinoside, in which all or most data points fell in the area of supra-additivity in all cell lines tested. The mean values of the observed data were significantly smaller than those of the predicted minimum values for the additive effect, indicating a synergistic effect of the two drugs (Table 1). The combination of bendamustine and two other pyrimidine analogues, gemcitabine and decitabine, produced virtually identical results, whereas the combination with a purine analogue F-Ara-A was only additive (Table 1). The combination of bendamustine and topoisomerase inhibitors (doxorubicin, mitoxantrone and etoposide) yielded additive effects in all cell lines examined (Figure 2C and Table 1). It is of note that bendamustine and bortezomib made favorable combinations (Table 1). In contrast, methotrexate was quite antagonistic with bendamustine (Figure 2D and Table 1). These results suggest that alkylating agents and pyrimidine analogues are suitable drugs to be combined with bendamustine for the treatment of intractable lymphoid malignancies.

Cell Cycle Effects of the Combination of Bendamustine with Cyclophosphamide or Cytosine Arabinoside

Next, we attempted to clarify the mechanisms by which alkylating agents and pyrimidine analogues are synergistic with bendamustine. Toward this end, we first performed cell cycle analysis of HBL-2 cells treated with bendamustine in combination with either 4-OHCY or cytosine arabinoside. Bendamustine alone arrested target cells in the late S phase, whereas cytosine arabinoside caused early S-phase block in HBL-2 cells (Figure 3A). The combination of the two drugs induced a decrease in late S-phase cells with massive apoptosis. As shown in Figure 3B, 4-OHCY alone arrested cells in mid- to late S phase 48 hours after culture. Simultaneous addition of bendamustine and 4-OHCY enhanced S-phase arrest, followed by an increase in the size of sub-G1 fractions. The results of cell cycle analysis imply that bendamustine and 4-OHCY exert synergistic effects by activating the same pathway, probably DNA damage response, leading to enhanced S-phase arrest and apoptosis, whereas bendamustine and cytosine arabinoside might potentiate each other in different ways to yield synergism.

Bendamustine Elicits DNA Damage Response and Subsequent Apoptosis Faster and with a Shorter Exposure Time than other Alkylating Agents

If bendamustine and 4-OHCY could exert synergistic effects by enhancing the same pathway, this might be linked to the ability of bendamustine to induce DNA damage (S-phase arrest) and apoptosis rapidly, as shown in Figure 1B. To confirm this hypothesis, we investigated whether bendamustine indeed activates DNA damage response faster than other alkylating agents. For this purpose, we compared the kinetics of checkpoint kinase activation by bendamustine with that of 4-OHCY. As shown in Figure 4A, bendamustine induced marked phosphorylation of checkpoint kinases Chk1 and Chk2 in HBL-2 and Namalwa cells at early time points (3–18 hours), whereas the equitoxic dose of 4-OHCY failed to do so at the same time points. In bendamustine-treated cells, Chk1 and Chk2 phosphorylation peaked at 9–18 hours, whereas it peaked after 48 hours with 4-OHCY treatment at equitoxic concentrations. To confirm the above finding, we cultured HBL-2 and Namalwa cells with various concentrations of bendamustine and 4-OHCY for 12 hours and found that bendamustine induced stronger phosphorylation than 4-OHCY in an equitoxic range (Figure 4B). In support of these observations, bendamustine induced the phosphorylation of ATM and p53 markedly and ATR slightly in HBL-2 cells after 6 and 3 hours, respectively, whereas 4-OHCY induced very weak or negligible phosphorylation of DNA damage response proteins under the same condition (Figure S2). Furthermore, we examined the phosphorylation of Chk1 and Chk2 in HBL-2 and Namalwa cells treated with IC50 values of various anti-cancer agents for 6 hours. As shown in Figure 4C, bendamustine readily induced the phosphorylation of Chk1 and Chk2, whereas other drugs could

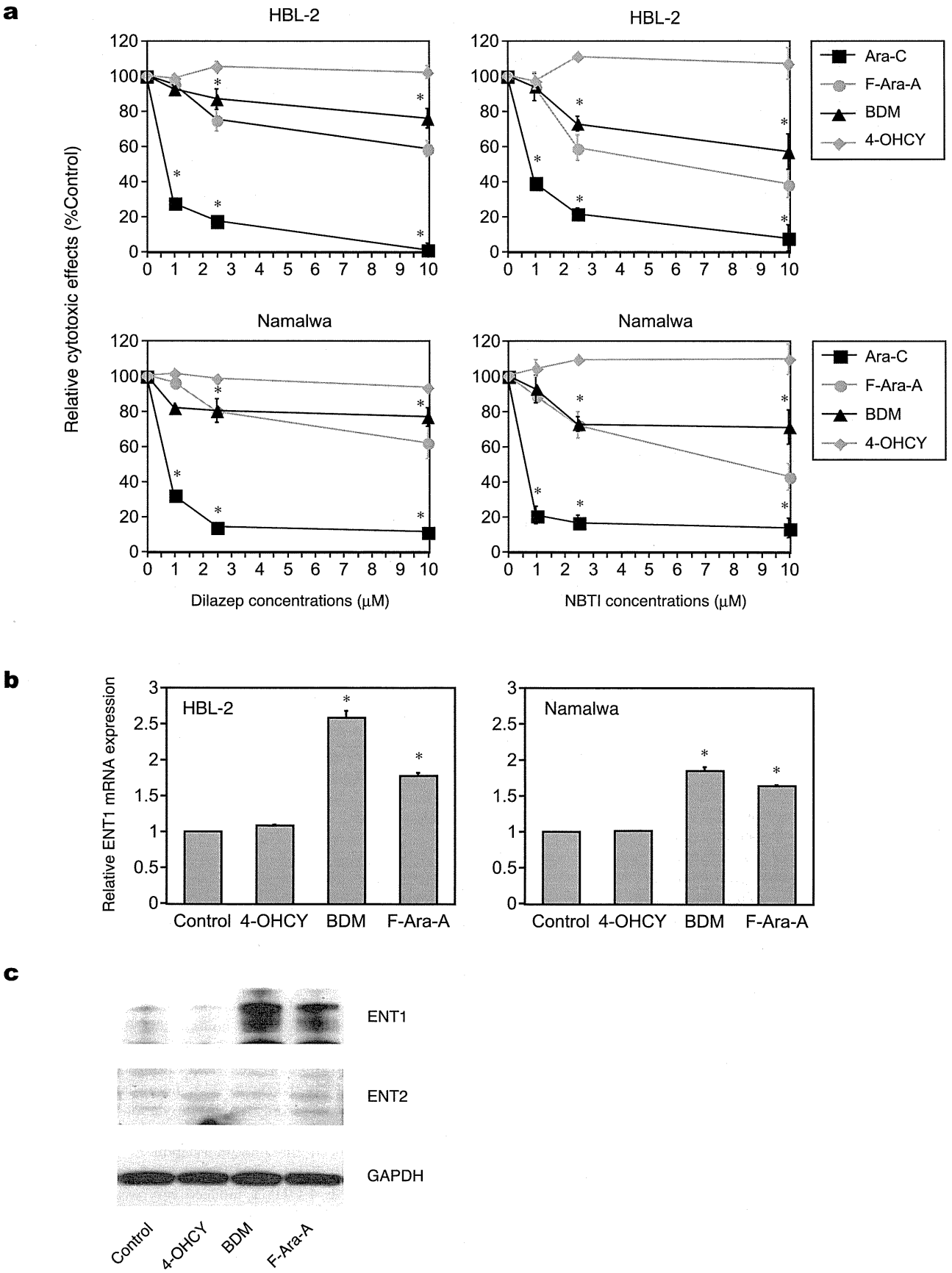

Figure 5. Purine analog-like properties of bendamustine. (A) Effects of dilazep (left panel) and NBTI (right panel) on cytotoxicity of the indicated drugs at IC50 against HBL-2 (upper panel) and Namalwa (lower panel) cells. (B) *ENT1* mRNA expression in HBL-2 and Namalwa cells treated

with the indicated drugs. The y-axes indicate relative gene expression against the expression levels of the untreated control being set at 1.0. The means ± S.D. (bars) of three independent experiments are shown. *P*-values were calculated by one-way ANOVA with the Student-Newman-Keuls multiple comparisons test. Asterisks denote $p<0.05$ against the untreated control. (C) HBL-2 and Namalwa cells were cultured in the absence (Control) or presence of IC50 values of the indicated drugs. Whole cell lysates were isolated after 48 hours and subjected to immunoblot analysis for the expression of ENT1, ENT2 and GAPDH (internal control). The data shown are representative of multiple independent experiments.
doi:10.1371/journal.pone.0090675.g005

not provoke comparable levels of phosphorylation at this time point.

These results indicate that bendamustine can rapidly induce irreparable DNA damage, thereby triggering Chk1- and Chk2-dependent apoptosis faster than other alkylating agents. To corroborate this assumption, we performed wash-out experiments and found that only 3-hour exposure was sufficient for bendamustine to elicit full cytotoxic activity in HBL-2 cells (Figure 4D, left panel), whereas 4-OHCY required at least 12-hour exposure (Figure 4D, right panel). These observations suggest that the exposure time required for commitment to cell death is very short for bendamustine, explaining the additive effects of bendamustine and other alkylating agents; DNA damage rapidly provoked by the former (within 24 hours) is boosted later by the latter (after 48 hours). However, additional evidence is required to explain the synergism between bendamustine and other alkylators. Nonetheless, an emerging question here is why bendamustine can induce DNA damage more rapidly than other alkylating agents.

Purine Analog-like Properties Underlie Rapid Induction of DNA Damage and Synergistic Effects with Pyrimidine Analogues

Rapid uptake of the drug may provide a good explanation for the rapid induction of DNA damage by bendamustine. In general, uptake of alkylating agents is mediated through simple passive diffusion [40,41]. In addition to simple passive diffusion, bendamustine uptake might be facilitated via nucleoside transporters

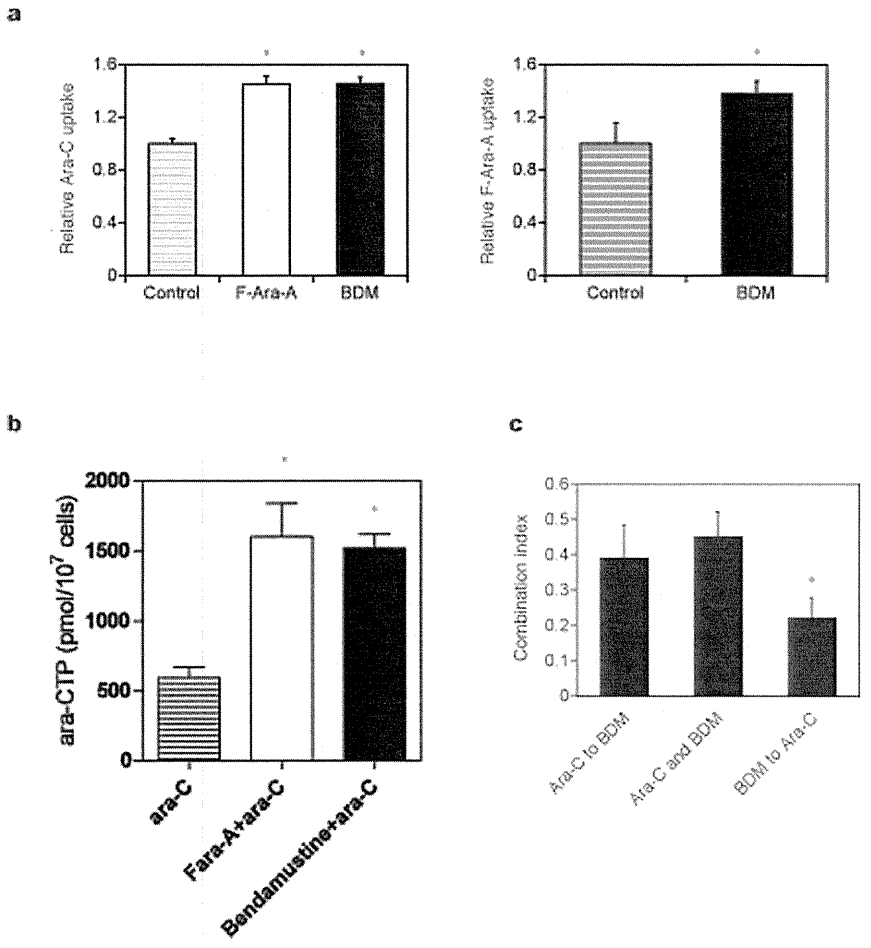

Figure 6. Bendamustine enhances the uptake of Ara-C and subsequent increase in Ara-CTP in HBL-2 cells. (A) HBL-2 cells were pretreated with the vehicle alone (Control), F-Ara-A or bendamustine (BDM), followed by the incubation with either [5-^{3}H]Ara-C (left panel) and [8-^{3}H]F-Ara-A (right panel). Drug incorporation was estimated by counting radioactivity of the nucleotide pool. (B) HBL-2 cells were pretreated with the vehicle alone (ara-C), F-Ara-A (F-ara-A+ara-C) or bendamustine (Bendamustine+ara-C), followed by the incubation with Ara-C. Intracellular Ara-CTP levels were determined using HPLC as described in Materials and Methods. (C) HBL-2 cells were treated with Ara-C and bendamustine (BDM) under three different conditions as described in Materials and Methods and subjected to isobologram analysis to compare the combination index. The means ± S.D. (bars) of three independent experiments are shown. *P*-values were calculated by one-way ANOVA with the Student-Newman-Keuls multiple comparisons test. Asterisks denote $p<0.05$ against the untreated control.
doi:10.1371/journal.pone.0090675.g006

because of its purine-like structure [42,43]. This possibility was proposed in a preliminary study [44], but has not been confirmed to date. We tested this possibility using dilazep, a potent inhibitor of both equilibrative nucleoside transporter 1 (ENT1) and ENT2, and NBTI, a specific inhibitor of ENT1 (33, 42, 43). As anticipated, both dilazep and NBTI almost completely abrogated the cytotoxic effect of cytosine arabinoside against HBL-2 and Namalwa cells, whereas they did not affect the activity of 4-OHCY at all (Figure 5A). Under the same experimental condition, the effect of bendamustine was slightly but significantly ameliorated by both inhibitors to a similar extent as that of a *bona fide* purine analog F-Ara-A. These results suggest that cellular uptake of bendamustine is at least partly mediated through nucleoside transporters, which enable rapid internalization and activation of DNA damage response.

It is well known that purine analogs potentiate the activity of cytosine arabinoside by increasing intracellular concentrations of the drug and its active metabolite Ara-CTP [45,46]. In addition, Petersen et al. [47] reported that purine analogs auto-enhanced the cytotoxic effects by up-regulating the expression of nucleoside transporters in CLL cells. From these observations, we reasoned that bendamustine exerts synergistic effects with pyrimidine analogues via modulation of ENT expression. As shown in Figure 5B and 5C, bendamustine readily increased the expression of ENT1 but not ENT2 at both mRNA and protein levels to an extent comparable with F-Ara-A. In accord with the increased expression of ENT1, cellular uptake of its substrates, cytosine arabinoside and F-Ara-A, was significantly enhanced by pretreatment with bendamustine (Figure 6A). Furthermore, bendamustine actually increased the intracellular concentration of Ara-CTP, an active metabolite of cytosine arabinoside, in HBL-2 cells (Figure 6B). If bendamustine potentiates the activity of cytosine arabinoside by enhancing the expression of ENT1, pretreatment with bendamustine produces more potent effects than simultaneous addition of both agents. The results shown in Figure 6C indicate that this is really the case; sequential addition of bendamustine followed by cytosine arabinoside yielded significantly stronger synergism than simultaneous addition of both agents and sequential addition of cytosine arabinoside followed by bendamustine.

Discussion

The efficacy of bendamustine monotherapy and its combination with rituximab has been established in the treatment of CLL and untreated indolent lymphomas [8,11]; however, combined therapy with other therapeutic agents might be required for the treatment of relapsed cases and intractable malignancies such as mantle cell lymphoma, DLBCL, aggressive lymphomas and multiple myeloma, all of which are relatively resistant to bendamustine. In this study, we therefore investigated the interactions between bendamustine and 13 drugs that represent six different classes of cytotoxic agents commonly used for the treatment of lymphoid malignancies in cell lines derived from bendamustine-resistant entities. We found that bendamustine yielded particularly effective combinations with alkylating agents (4-hydroperoxy-cyclophosphamide, chlorambucil and melphalan) and pyrimidine analogues (cytosine arabinoside, gemcitabine and decitabine), and determined that purine analog-like properties of bendamustine underlie the synergic interactions.

As it is widely believed that bendamustine primarily functions as an alkylating agent, the synergistic effect with other alkylators seems to be unreasonable. We propose different kinetics of the DNA damage response as a mechanism of favorable combination. Bendamustine is rapidly incorporated into target cells through nucleoside transporters, probably because of its purine-like structure, thereby inducing DNA damage significantly faster than others. DNA damage rapidly provoked by bendamustine could be boosted later by other alkylating agents. Moreover, biological half-lives of bendamustine and cyclophosphamide are 49.1 and 311.4 minutes, respectively [38,39,48]. Therefore, rapid transport of bendamustine is advantageous for active forms to be accumulated in target cells more efficiently, resulting in rapid and robust induction of DNA damage, followed by the effects of other agents with longer half-lives such as cyclophosphamide. Although this scenario may explain additive effects, further investigation is required to understand the mechanism of the synergism between bendamustine and other alkylating agents.

The purine analog-like properties of bendamustine also provide a good explanation for its synergistic effects with pyrimidine analogues. Purine analogs are known to potentiate the activity of cytosine arabinoside by increasing intracellular concentrations of the drug and its active metabolite Ara-CTP via inhibition of ribonucleotide reductase [45,46] and enhancement of ENT expression [47]. We found that bendamustine also induced the up-regulation of ENT1 expression and an increase in Ara-CTP in target cells, which underlies the synergistic effects with bendamustine and cytosine arabinoside. Simultaneous addition of bendamustine and F-Ara-A, another substrate of ENT1, yielded only an additive effect in isobologram analysis. This may be due to the competition of the two agents for ENT1, because pretreatment with bendamustine significantly enhanced the accumulation of F-Ara-A, which administered later, in HBL-2 cells. It is of note that bendamustine-induced increase in ENT1 expression occurs at mRNA levels. This is compatible with the results of a previous Gene Ontology study, in which bendamustine could up-regulate the expression of multiple and distinct sets of genes, including those related to nucleobase, nucleoside, nucleotide and nucleic acid metabolism, compared with other alkylating agents [4]. The mechanisms underlying the up-regulation of ENT1 transcripts by bendamustine are currently under investigation in our laboratory.

Some clinical trials have documented the efficacy of the combination of bendamustine and other drugs, such as mitoxantrone, fludarabine, cytosine arabinoside, vincristine and corticosteroids, for patients with relapsed and/or refractory lymphoid malignancies [25–28,49]. Among them, the combination of bendamustine with cytosine arabinoside (R-BAC therapy) showed a remarkable therapeutic impact with moderate toxicity on patients with CLL and mantle cell lymphoma ineligible for intensive treatments [27,28]. The synergistic effect of bendamustine and cytosine arabinoside is fully consistent with our observation and others [22,23]. Furthermore, in the R-BAC regimen, sequential treatment with bendamustine first followed by cytosine arabinoside was proven to be more effective than simultaneous addition of the two drugs. This clinical fact is well supported by our experimental findings. In addition, the combination of bendamustine with cytosine arabinoside and melphalan (BeEAM) is highly efficacious as a conditioning regimen to stem cell transplantation for heavily treated patients with Hodgkin lymphoma, DLBCL and mantle cell lymphoma [50]. Undoubtedly, such effective regimens are in high demand for intractable malignancies including mantle cell lymphoma and multiple myeloma. The present findings provide a theoretical basis for the development of more effective bendamustine-based combination therapies.

Supporting Information

Figure S1 Schematic representation of the isobologram of Steel and Peckham. Envelope of additivity, surrounded by Mode I (solid line) and Mode II (dotted lines) isobologram lines, was constructed from the dose-response curves of bendamustine and a combined drug. The concentrations that produced 80% or 50% growth inhibition were expressed as 1.0 on the ordinate and the abscissa of isobolograms. Combined data points Pa, Pb, Pc and Pd represent supra-additive, additive, sub-additive and protective effects, respectively.
(TIF)

Figure S2 Time-course analysis of ATM, ATR and p53 phosphorylation in HBL-2 cells treated with IC50 values of bendamustine or 4-OHCY. We used specific antibodies against phosphorylated p53 at Ser-15, phosphorylated ATM at Ser-1981 and phosphorylated ATR at Ser-428 (Cell Signaling Technology). The membranes were reblotted with anti-GAPDH antibody to serve as an internal control.
(TIF)

Acknowledgments

The authors are indebted to Professor Martin J.S. Dyer (MRC Toxicology Unit, Leicester University, Leicester, UK) for providing Granta 519 and NCEB-1 cell lines.

Author Contributions

Conceived and designed the experiments: NH JK YK YF. Performed the experiments: NH JK TY DK TW MU MA YK YF. Analyzed the data: NH JK TY DK TW TU YK YF. Contributed reagents/materials/analysis tools: SM YN. Wrote the paper: NH JK TY TU YK YF.

References

1. Tageja N, Nagi J (2010) Bendamustine: something old, something new. Cancer Chemother Pharmacol 66: 413–423.
2. Hartmann M, Zimmer C (1972) Investigation of cross-link formation in DNA by the alkylating cytostatic IMET 3106, 3393 and 3943. Biochim Biophys Acta 287: 386–389.
3. Strumberg D, Harstrick A, Doll K, Hoffmann B, Seeber S (1996) Bendamustine hydrochloride activity against doxorubicin-resistant human breast carcinoma cell lines. Anticancer Drugs 7: 415–421.
4. Leoni LM, Bailey B, Reifert J, Bendall HH, Zeller RW, et al. (2008) Bendamustine (Treanda) displays a distinct pattern of cytotoxicity and unique mechanistic features compared with other alkylating agents. Clin Cancer Res 14: 309–317.
5. Schwänen C, Hecker T, Hübinger G, Wölfle M, Ritgen W, et al. (2002) In vitro evaluation of bendamustine induced apoptosis in B-chronic lymphocytic leukemia. Leukemia 16: 2096–2105.
6. Roué G, López-Guerra M, Milpied P, Pérez-Galán P, Villamor N, et al. (2008) Bendamustine is effective in p53-deficient B-cell neoplasms and requires oxidative stress and caspase-independent signaling. Clin Cancer Res 14: 6907–6915.
7. Becharry N, Rattner JB, Bellacosa A, Smith MR, Yen TJ (2012) Dose dependent effects on cell cycle checkpoints and DNA repair by bendamustine. PLoS ONE 7: e40342.
8. Knauf WU, Lissichkov T, Aldaoud A, Liberati A, Loscertales J, et al. (2009) Phase III randomized study of bendamustine compared with chlorambucil in previously untreated patients with chronic lymphocytic leukemia. J Clin Oncol 27: 4378–4384.
9. Friedberg JW, Cohen P, Chen L, Robinson KS, Forero-Torres A, et al. (2008) Bendamustine in patients with rituximab-refractory indolent and transformed non-Hodgkin's lymphoma: results from a phase II multicenter, single-agent study. J Clin Oncol 26: 204–210.
10. Robinson KS, Williams ME, van der Jagt RH, Cohen P, Herst JA, et al. (2008) Phase II multicenter study of bendamustine plus rituximab in patients with relapsed indolent B-cell and mantle cell non-Hodgkin's lymphoma. J Clin Oncol 26: 4473–4479.
11. Rummel MJ, Niederle N, Maschmeyer G, Banat GA, von Grünhagen U, et al. (2013) Bendamustine plus rituximab versus CHOP plus rituximab as first-line treatment for patients with indolent and mantle-cell lymphomas: an open-label, multicetre, randomised, phase 3 non-inferiority trial. Lancet 381: 1203–1210.
12. Ohmachi K, Niitsu N, Uchida T, Kim SJ, Ando K, et al. (2013) Multicenter phase II study of bendamustine plus rituximab in patients with relapsed or refractory diffuse large B-cell lymphoma. J. Clin Oncol 31: 2103–2109.
13. McCloskey JK, Broome CM, Cheson BD (2013) Safe and effective treatment of aggressive non-Hodgkin lymphoma with rituximab and bendamustine in patients with severe liver impairment. Clin Adv Hematol Oncol 11: 184–188.
14. Hitz F, Fisher N, Pabst Th, Casper C, Berthod G, et al. (2013) Rituximab, bendamustine, and lenalidomide in patients with aggressive B cell lymphoma not eligible for high-dose chemotherapy or anthracycline-based therapy: phase I results of the SAKK 38/08 trial. Ann Hematol 92: 1033–1040.
15. Lentzsch S, O'Sullivan A, Kennedy RC, Abbas M, Dai L, et al. (2012) Combination of bendamustine, lenalidomide, and dexamethasone (BLD) in patients with relapsed or refractory multiple myeloma is feasible and highly effective: results of phase 1/2 open-label, dose escalation study. Blood 119: 4608–4613.
16. Offidani M, Corvatta L, Maracci L, Liberati AM, Ballanti S, et al. (2013) Efficacy and tolerability of bendamustine, bortezomib and dexamethasone in patients with relapsed-refractory multiple myeloma: a phase II study. Blood Cancer J 3: e162.
17. Damaj G, Gressin R, Bouabdallah K, Cartron G, Choufi B, et al. (2013) Results from a prospective, open-label, phase II trial of bendamustine in refractory or relapsed T-cell lymphomas: the BENTLY trial. J Clin Oncol 31: 104–110.
18. Köster W, Stamatis G, Heider A, Avramidis K, Wilke H, et al. (2004) Carboplatin in combination with bendamustine in previously untreated patients with extensive-stage small cell lung cancer (SCLC). Clin Drug Investig 24: 611–618.
19. Layman RM, Ruppert AS, Lynn M, Mrozek E, Ramaswamy B, et al. (2013) Severe and prolonged lymphopenia observed in patients treated with bendamustine and erlotinib for metastatic triple negative breast cancer. Cancer Chemother Pharmacol 71: 1183–1190.
20. Chow KU, Boehrer S, Geduldig K, Krapohl A, Hoelzer D, et al. (2001) *In vitro* induction of apoptosis of neoplastic cells in low-grade non-Hodgkin's lymphomas using combinations of established cytotoxic drugs with bendamustine. Haematologica 86: 485–493.
21. Chow KU, Noval D, Boehrer S, Ruthardt M, Knau A, et al. (2003) Synergistic effects of chemotherapeutic drugs in lymphoma cells are associated with down-regulation of inhibitor of apoptosis proteins (IAPs), prostate-apoptosis-response-gene 4 (Par-4), death-associated protein (Daxx) and with enforced caspase activation. Biochem Pharmacol 66: 711–724.
22. Castegnaro S, Visco C, Chieregato K, Bernardi M, Albiero E, et al. (2012) Cytosine arabinoside potentiates the apoptotic effect of bendamustine on several B- and T-cell leukemia/lymphoma cells and cell lines. Leuk Lymphoma 53: 2262–2258.
23. Visco C, Castegnaro S, Chieregato K, Bernardi M, Albiero E, et al. (2012) The cytotoxic effects of bendamustine in combination with cytarabine in mantle lymphoma cell lines. Blood Cell Mol Dis 48: 68–75.
24. Cai B, Lyu H, Huang J, Wang S, Lee CK, et al. (2013) Combination of bendamustine and entinostat synergistically inhibits proliferation of multiple myeloma cells via induction of apoptosis and DNA damage response. Cancer Lett 335: 343–350.
25. Koenigsmann M, Knauf W, Herold M, Pasold R, Müller G, et al. (2004) Fludarabine and bendamustine in refractory and relapsed indolent lymphoma - multicenter phase I/II trial of the East German Society of Hematology and Oncology (OSHO). Leuk Lymphoma 45: 1821–1827.
26. Weide R, Hess G, Köppler H, Heymanns J, Thomalla J, et al. (2007) German Low Grade Lymphoma Study Group: High anti-lymphoma activity of bendamustine/mitoxantrone/rituximab in rituximab pretreated relapsed or refractory indolent lymphomas and mantle cell lymphomas. A multicenter phase II study of the German Low Grade Lymphoma Study Group (GLSG). Leuk Lymphoma 48: 1299–1306.
27. Visco C, Finotto S, Zambello R, Paolini R, Menin A, et al. (2013) Combination of rituximab, bendamustine, and cytarabine for patients with mantle-cell non-Hodgkin lymphoma ineligible for intensive regimens or autologous transplantation. J Clin Oncol 31: 1442–1449.
28. Visco C, Finotto S, Pomponi F, Sartoli R, Laveder F, et al. (2013) The combination of rituximab, bendamustine, and cytarabine for heavily pretreated relapsed/refractory cytogenetically high-risk patients with chronic lymphocytic leukemia. Am J Hematol 88: 289–293.
29. Abe M, Nozawa Y, Wakasa H, Ohno H, Fukuhara S (1988) Characterization and comparison of two newly established Epstein-Barr virus-negative lymphoma B-cell lines. Surface markers, growth characteristics, cytogenetics, and transplantability. Cancer 61: 483–490.
30. Hiraoka N, Kikuchi J, Koyama D, Wada T, Mori S, et al. (2013) Alkylating agents induce histone H3K18 hyperacetylation and potentiate HDAC inhibitor-mediated global histone acetylation and cytotoxicity in mantle cell lymphoma. Blood Cancer J 3: e169.
31. Furukawa Y, Vu HA, Akutsu M, Odgerel T, Izumi T, et al. (2007) Divergent cytotoxic effects of PKC412 in combination with conventional antileukemic

agents in FLT3 mutation-positive versus -negative leukemia cell lines. Leukemia 21: 1005–1014.
32. Koyama D, Kikuchi J, Hiraoka N, Wada T, Kurosawa H, et al. (2014) Proteasome inhibitors exert cytotoxicity and increase chemosensitivity via transcriptional repression of Notch1 in T-cell acute lymphoblastic leukemia. Leukemia, advanced online publication, 17 January 2014; doi:10.1038/leu.2013.366.
33. Wright AMP, Gati WP, Paterson ARP (2000) Enhancement of retention and cytotoxicity of 2-chlorodeoxyadenosine in cultured human leukemic lymphoblasts by nitrobenzylthioinosine, an inhibitor of equilibrative nucleoside transport. Leukemia 14: 52–60.
34. Kikuchi J, Yamada S, Koyama D, Wada T, Nobuyoshi M, et al. (2013) The novel orally active proteasome inhibitor K-7174 exerts anti-myeloma activity *in vitro* and *in vivo* by down-regulating the expression of class I histone deacetylases. J Biol Chem 288: 25593–25602.
35. Yamauchi T, Negoro E, Kishi S, Takagi K, Yoshida A, et al. (2009) Intracellular cytarabine triphosphate production correlates to deoxycytidine kinase/cytosolic 5′-nucleotidase II expression ratio in primary acute myeloid leukemia cells. Biochem Pharmacol 77: 1780–1786.
36. Yamauchi T, Ueda T (2005) A sensitive new method for clinically monitoring cytarabine concentrations at the DNA level in leukemia cells. Biochem Pharmacol 69: 1795–1803.
37. Yamauchi T, Ueda T, Nakamura T (1996) A new sensitive method for determination of intracellular 1-ß-D-arabinofuranosylcytosine 5′-triphosphate content in human materials *in vivo*. Cancer Res 56: 1800–1804.
38. Rasschaert M, Schrijvers D, Van den Brande J, Dyck J, Bosmans J, et al. (2007) A phase I study of bendamustine hydrochloride administered day 1+2 every 3 weeks in patients with solid tumours. Br J Cancer 96: 1692–1698.
39. Ogura M, Uchida T, Taniwaki M, Ando K, Watanabe T, et al. (2010) Phase I and pharmacokinetic study of bendamustine hydrochloride in relapsed or refractory indolent B-cell non-Hodgkin lymphoma and mantle cell lymphoma. Cancer Sci 101: 2054–2058.
40. Hill BT (1972) Studies on the transport and cellular distribution of chlorambucil in the Yoshida ascites sarcoma. Biochem Pharmacol 21: 495–502.
41. Boyd VL, Robbins JD, Egan W, Ludeman SM (1986) ^{31}P nuclear magnetic resonance spectroscopic observation of the intracellular transformations of oncostatic cyclophosphamide metabolites. J Med Chem 29: 1206–1210.
42. Pastor-Anglada M, Molina-Arcas M, Casado FJ, Bellosillo B, Colomer D, et al. (2004) Nucleoside transporters in chronic lymphocytic leukemia. Leukemia 18: 385–393.
43. Fernandez-Calotti PX, Colomer D, Pastor-Anglada M (2011) Translocation of nucleoside analogs across the plasma membrane in hematologic malignancies. Nucleosides, Nucleotides and Nucleic Acids 30: 1324–1340.
44. Staib P, Schinköthe T, Dimski T, Lathan B, Boos J, et al. (1999) In-vitro modulation of Ara-CTP accumulation in fresh AML cells by bendamustine in comparison with fludarabine, 2-CDA and gemcitabine. Blood 94: 63a.
45. Gandhi V, Estey E, Keating MJ, Chucrallah A, Plunkett W (1996) Chlorodeoxyadenosine and arbinosylcytosine in patients with acute myelogenous leukemia: Pharmacokinetic, pharmacodynamic, and molecular interactions. Blood 87: 256–264.
46. Chow KU, Boehrer S, Napieralski S, Novak D, Knau A, et al. (2003) In AML cell lines Ara-C combined with purine analogues is able to exert synergistic as well as antagonistic effects on proliferation, apoptosis and disruption of mitochondrial membrane potential. Leuk Lymphoma 44: 165–173.
47. Petersen AJ, Brown RD, Gibson J, Pope B, Luo XF, et al. (1996) Nucleoside transporters, bcl-2 and apoptosis in CLL cells exposed to nucleoside analogues *in vitro*. Eur J Haematol 56: 213–220.
48. Chan KK, Hong PS, Tutsch K, Trump DL (1994) Clinical pharmacokinetics of cyclophosphamide and metabolites with and without SR-2508. Cancer Res 54: 6421–6429.
49. Herold M, Schulze A, Niederwieser D, Franke A, Fricke HJ, et al. (2006) Bendamustine, vincristine and prednisone (BOP) versus cyclophosphamide, vincristine and prednisone (COP) in advanced indolent non-Hodgkin's lymphoma and mantle cell lymphoma: results of a randomised phase III trial (OSHO# 19). J Cancer Res Clin Oncol 132: 105–112.
50. Visani G, Malerba L, Stefani PM, Capria S, Galieni P, et al. (2011) BeEAM (bendamustine, etoposide, cytarabine, melphalan) before autologous stem cell transplantation is safe and effective for resistant/relapsed lymphoma patients. Blood 118: 3419–3425.

OPEN

Citation: Blood Cancer Journal (2013) **3**, e169; doi:10.1038/bcj.2013.66

www.nature.com/bcj

LETTER TO THE EDITOR

Alkylating agents induce histone H3K18 hyperacetylation and potentiate HDAC inhibitor-mediated global histone acetylation and cytotoxicity in mantle cell lymphoma

Blood Cancer Journal (2013) **3,** e169; doi:10.1038/bcj.2013.66; published online 13 December 2013

Histone modifications have crucial roles in diverse biological processes including development, differentiation and oncogenesis. Among them, acetylation of histone H3 at the lysine-18 residue (H3K18) is particularly important, because specific deacetylation of H3K18 is indispensable for oncogenic transformation by adenovirus[1] and for host responses to bacterial infection.[2] Regarding the former, it has also been demonstrated that H3K18 hypoacetylation is linked to the maintenance of malignant phenotypes[3] and poor prognosis[4,5] in cancer.

Given the fundamental roles of H3K18 hypoacetylation in cancer biology, we investigated the possibility of therapeutic targeting of this modification in mantle cell lymphoma (MCL), in which epigenetic alterations, including aberrant hypomethylation of the *HDAC1* gene,[6] are central to the disease process and in which conventional therapies are usually not effective.[7] Toward this end, we first screened for the effects of various anti-cancer drugs on the levels of H3K18 acetylation in the MCL cell line HBL-2. As shown in Figure 1a, in addition to the HDAC inhibitor romidepsin, two alkylating agents, bendamustine and 4-hydroperoxy-cyclophosphamide (4-OHCY; an active metabolite of cyclophosphamide), were able to reverse H3K18 hypoacetylation, whereas doxorubicin, dexamethasone and chlorambucil failed to do so at equitoxic concentrations. The increase in the acetylation levels of H3K18 was time dependent and considerably sustained until cell death (~72 h; Figure 1b). This observation was reproducible in other MCL cell lines, except in Granta519, which is highly resistant to chemotherapeutic agents,[7] upon treatment

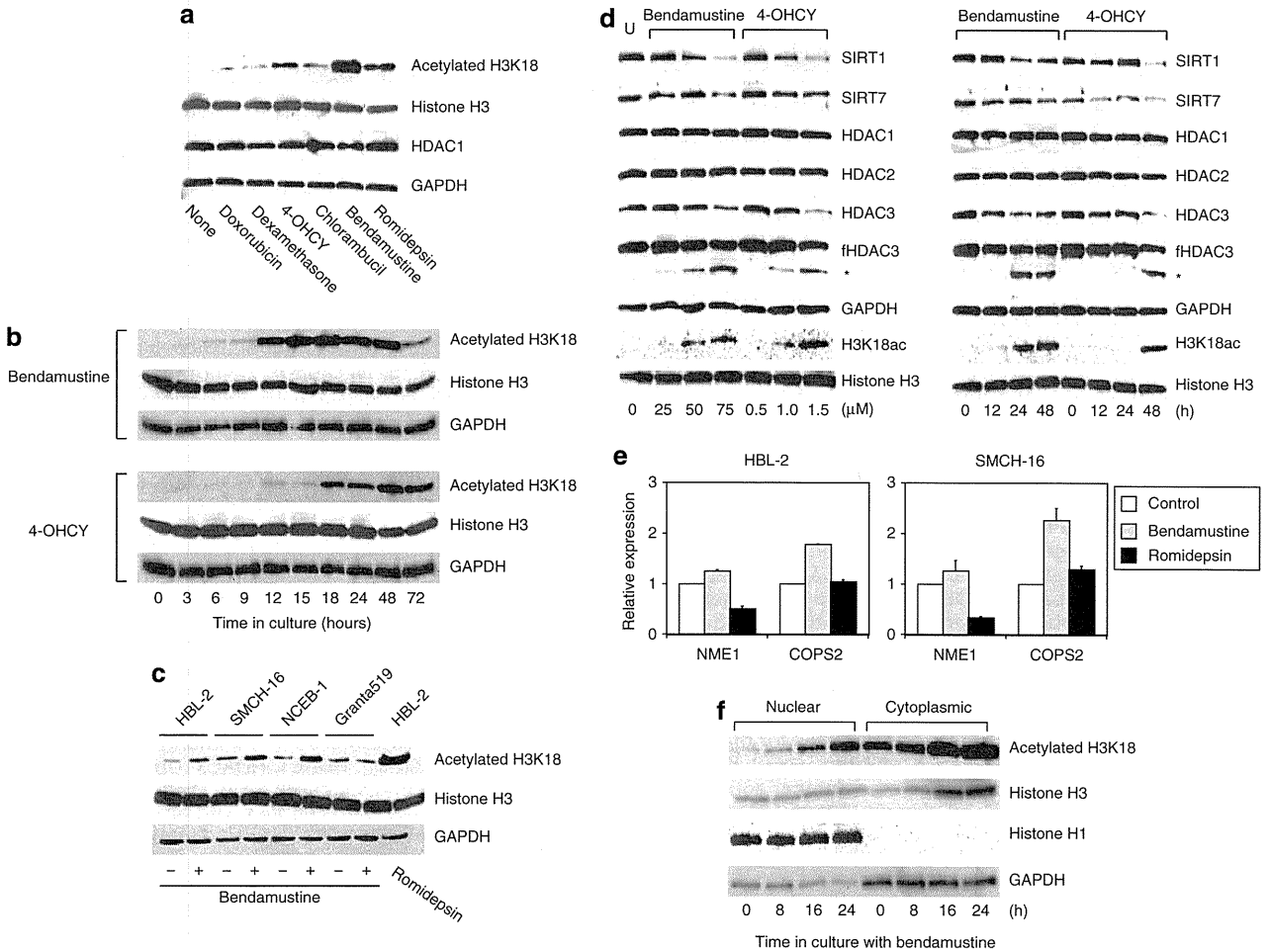

Figure 1. See next page for caption.

with bendamustine (Figure 1c). Moreover, we confirmed the induction of H3K18-specific acetylation in the bendamustine-sensitive Burkitt lymphoma cell line Namalwa but not in the bendamustine-resistant myeloid leukemia cell line K-562 (Supplementary Figure 1). It is of note that neither bendamustine nor 4-OHCY alone induced hyperacetylation at other sites including H3K9, H3K27, H4K5, H4K12 and H4K16 (Supplementary Figure 1).

Next, we sought to clarify the mechanisms by which bendamustine and 4-OHCY specifically enhanced H3K18 acetylation in target cells. A recent study by Barber *et al.*[3] indicated that SIRT7, a class III HDAC, is responsible for site-specific deacetylation at H3K18 in cancer cells. Consistent with their finding, both bendamustine and 4-OHCY were seen to reduce the expression levels of SIRT7 in a dose- and time-dependent manner in HBL-2 cells (Figure 1d). Another class III HDAC, SIRT1, was also markedly downregulated under the same condition (Figure 1d), whereas there were no changes in the expression of SIRT2 and SIRT6 (data not shown). In addition, the two drugs decreased the abundance of full-length HDAC3 (~49 kDa) concomitantly with the appearance of the cleaved form (~42 kDa), whereas they did not affect the expression and activities of HDAC1 and HDAC2 (Figure 1d and data not shown). It is worth noting that the abundance of cleaved HDAC3 correlated precisely with the increase in H3K18 acetylation (Figure 1d).

Bendamustine-mediated H3K18 hyperacetylation might cause upregulation of a unique subset of target genes. Indeed, Barber *et al.*[3] reported that SIRT7-mediated hypoacetylation of H3K18 contributes to cancer development and maintenance through silencing of tumor suppressor genes such as *NME1* and *COPS2*. As anticipated, bendamustine increased the expression of these genes stronger than did romidepsin, which could not inhibit SIRT7 activity, in HBL-2 and SMCH-16 cells in association with the induction of H3K18 hyperacetylation (Figure 1e).

It is well known that core histones are acetylated immediately after translation in the cytoplasm and deacetylation allows their nuclear import by facilitating the binding of specific transporters to positively charged N-termini.[8] It is possible that, as a reciprocal process, H3K18 hyperacetylation causes cytoplasmic translocation of nuclear histone H3. Immunoblot analyses of nuclear and cytoplasmic fractions of bendamustine-treated HBL-2 cells clearly demonstrated that this was the case (Figure 1f), which may contribute to growth inhibition because a ready supply of histones is required for the assembly of newly replicated DNA to complete S-phase progression. This is fully consistent with a recent report by Qian *et al.*,[9] in which core histones are acetylated upon DNA damage and transferred to the cytoplasm, where they are degraded by the PA200/Bim 10-containing proteasomes, to facilitate DNA repair. Taken together, these results suggest that the repression of SIRT7 and HDAC3 is mainly responsible for H3K18 hyperacetylation induced by the two alkylating agents and that downregulation of SIRT1, a nuclear and cytoplasmic deacetylase for H3K9 and H4K16 as well as multiple non-histone cytosolic proteins including p53, may be implicated in further modification of translocated histone H3 in the cytoplasm.

As bendamustine and 4-OHCY appear to suppress the expression of SIRT1, SIRT7 and HDAC3, the combination with authentic HDAC inhibitors, which primarily target the catalytic activity of class I HDACs especially HDAC1 and HDAC2,[10] may produce synergistic effects in terms of histone acetylation and overall cytotoxicity. To substantiate this hypothesis, we first checked the acetylation status of histone tails in MCL cell lines treated with romidepsin and bendamustine simultaneously. As anticipated, romidepsin enhanced bendamustine-induced H3K18 acetylation in HBL-2 and SMCH-16 but not in Granta519 cells (Figure 2a). In addition, the two drugs synergistically induced hyperacetylation of other sites such as histones H3K9, H4K5, H4K12 and H4K16 (Figure 2a and data not shown). Drug combination analysis with isobolograms revealed that bendamustine and 4-OHCY were additive to synergistic cytotoxicity in combination with romidepsin against HBL-2 cells, whereas the combination with vincristine was rather antagonistic *in vitro* (Figure 2b). Next, we confirmed the synergistic effects of alkylating agents and HDAC inhibitors *in vivo* using a mouse xenograft model of MCL. As shown in Figure 2c, the combination of cyclophosphamide and romidepsin significantly retarded the growth of HBL-2 cells inoculated subcutaneously into immunodeficient mice at concentrations that did not affect tumor growth as single agents. Because romidepsin almost equally inhibits the enzymatic activity of HDAC1, 2 and 3,[10] we attempted to clarify the direct target(s) responsible for the synergism with alkylating agents using knockdown approaches. shRNA against HDAC3 but not HDAC1 and 2 showed favorable effects in combination with bendamustine and 4-OHCY in HBL-2 and SMCH-16 cells (Figure 2d and data not shown), consistent with our finding that alkylating agents downregulated HDAC3 without affecting the expression and activities of HDAC1 and 2.

Among class I HDACs, HDAC3 has distinct properties despite evolutionarily conserved structures with other members.[10] For instance, it has been reported that HDAC3 has critical roles in tumor cell viability, chromosomal stability, S-phase progression and the DNA damage response.[11] Another unique feature of HDAC3 is conditional cleavage by extrinsic stimuli. Xia *et al.*[12]

Figure 1. Alkylating agents induce histone H3K18 hyperacetylation through SIRT7 downregulation and HDAC3 cleavage. (**a**) HBL-2 cells were cultured with the indicated drugs at IC50 (doxorubicin 20 nM, dexamethasone 100 nM, 4-OHCY 1 μM, chlorambucil 4 μM, bendamustine 50 μM and romidepsin 2 nM) for 24 h and subjected to immunoblotting with specific antibodies against the histone H3 acetylated at lysine-18 (Cell Signaling Technology, Beverly, MA, USA), total histone H3 (Cell Signaling Technology), HDAC1 (Sigma-Aldrich, St Louis, MO, USA) and GAPDH (Santa Cruz Biotechnology, Santa Cruz, CA, USA). (**b**) HBL-2 cells were cultured with either bendamustine (provided by SymBio Pharmaceuticals, Tokyo, Japan) or 4-OHCY (provided by Shionogi, Osaka, Japan) at IC50 (50 and 1.0 μM, respectively) for the indicated periods and subjected to immunoblotting with specific antibodies against the histone H3 acetylated at lysine-18 (H3K18), histone H3 and GAPDH (loading controls). (**c**) We cultured four MCL cell lines in the absence (−) or presence (+) of 50 μM bendamustine for 12 h and subjected them to immunoblotting with specific antibodies against histone H3 acetylated at lysine-18 (H3K18), histone H3 and GAPDH (loading controls). HBL-2 cells were treated with 2 nM romidepsin (provided by Gloucester Pharmaceuticals, Cambridge, MA, USA) for 12 h to serve as a positive control for H3K18 hyperacetylation.[14] (**d**) HBL-2 cells were cultured with either bendamustine or 4-OHCY at the indicated concentrations for 24 h (left panel) or at IC50 (50 and 1.0 μM, respectively) for the indicated periods (right panel) and subjected to immunoblotting with specific antibodies against SIRT1, SIRT7, HDAC2, acetylated H3K18, histone H3 (Cell Signaling Technology), HDAC1, HDAC3 (Upstate Biotechnology, Lake Placid, NY, USA) and GAPDH. We also used another anti-HDAC3 antibody (BD Transduction Laboratories, San Diego, CA, USA) to detect both full-length HDAC3 (fHDAC3) and cleaved HDAC3 (asterisk).[13] (**e**) HBL-2 and SMCH-16 cells were cultured with either bendamustine or romidepsin at IC50 (50 μM and 2 nM, respectively) for 24 h and subjected to real-time quantitative RT-PCR using the TaqMan Expression Assays (Hs02621161 for NME1 and Hs00182826 for COPS2). The data were quantified with the $2^{-\Delta\Delta Ct}$ method using simultaneously amplified GAPDH (Hs01922876) as a reference. The *y* axis indicates relative gene expression with the expression levels of untreated control cells being set at 1.0. (**f**) We cultured HBL-2 cells with 50 μM bendamustine for the indicated periods and separated nuclear and cytoplasmic fractions using the Nuclear Extraction Kit (Cayman Chemical Company, Ann Arbor, MI, USA) according to the manufacturer's instructions. We monitored the quality of separation using histone H1 and GAPDH as nuclear and cytoplasmic markers, respectively. The data shown are representative of multiple independent experiments.

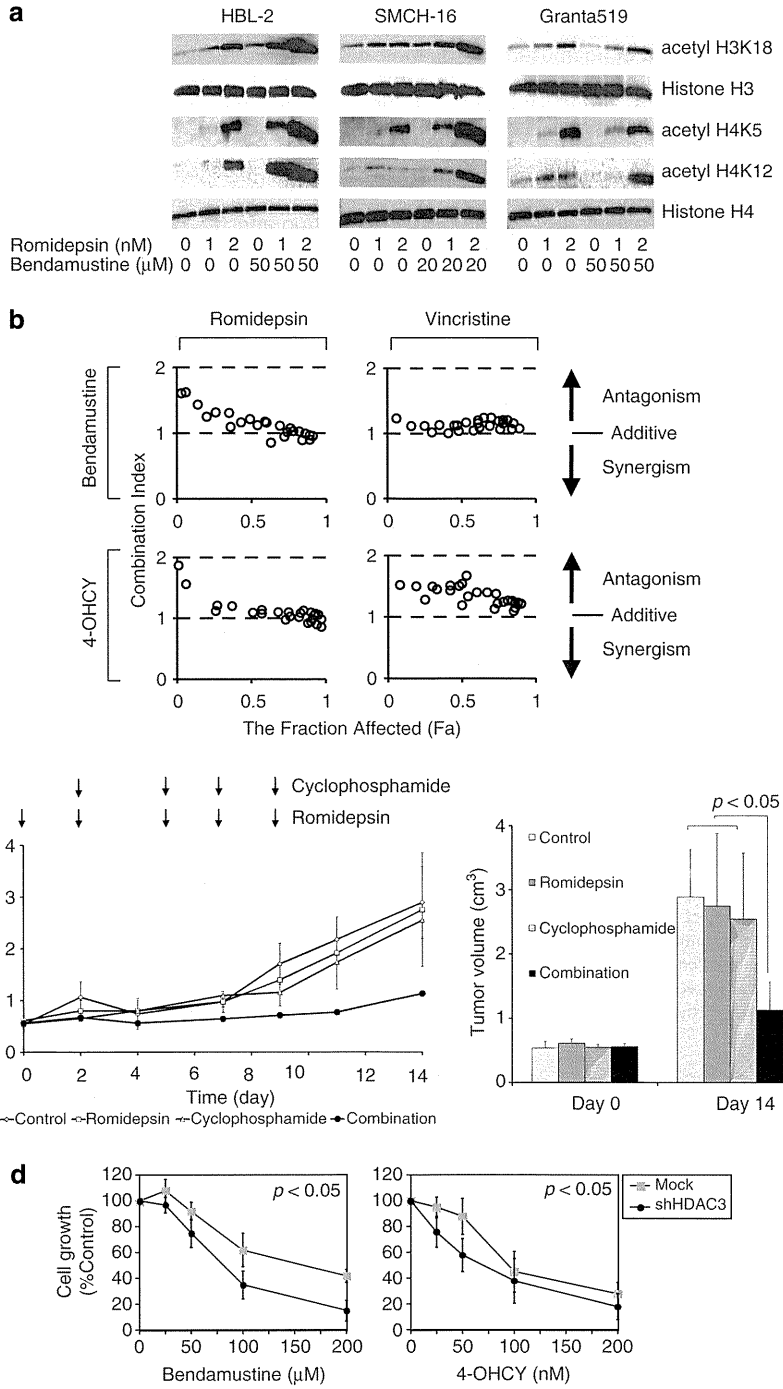

Figure 2. See next page for caption.

demonstrated that HDAC3 cleaved by osmotic stress is more active than full-length HDAC3 and decreases histone acetylation at promoter regions of the *c-Jun* gene. On the other hand, cleaved HDAC3 is exported to the cytoplasm during the apoptotic process because of the loss of nuclear localization signals, resulting in increased histone acetylation at promoter regions of apoptotic genes such as *Fas* and *Bax*, whereas global histone acetylation decreases probably because of concurrent inactivation of histone acetyltransferases.[13] In the present study, alkylator-cleaved HDAC3 remained in the nucleus (data not shown) but could not retain the ability of H3K18 deacetylation, implying that HDAC3 is inactivated by alkylating agents upon cleavage. These data suggest that alkylating agents cleave HDAC3 *via* distinct mechanisms from osmotic stress[12] and apoptotic insults such as Fas ligand and ultraviolet exposure.[13] The underlying mechanisms are currently under investigation in our laboratory.

In summary, this study uncovered a novel unexpected function of alkylating agents targeting cancer-specific histone modification (H3K18 hypoacetylation), which provides a rationale for the combination with HDAC inhibitors to potentiate each anti-tumor activity against intractable malignancies by epigenetic means, as exemplified here in MCL.

Figure 2. Alkylating agents potentiate HDAC inhibitor-mediated global histone hyperacetylation and cytotoxicity *in vitro* and *in vivo*. (**a**) MCL cell lines were cultured with romidepsin and bendamustine at the indicated concentrations for 12 h, and were subjected to immunoblotting using specific antibodies against acetylated histones H3K18, H4K5 and H4K12 (Cell Signaling Technology) and histone H3 and histone H4 (loading controls). (**b**) We treated HBL-2 cells with variable concentrations of bendamustine or 4-OHCY in combination with romidepsin or vincristine for 48 h and determined cell viability by the reduction of 3-(4,5-dimethylthiazol-2-yl)-2,5-diphenyltetrazolium bromide (MTT) using the Cell Counting Kit-8 (Wako Biochemicals, Osaka, Japan). We calculated the combination index of two anti-cancer drugs using CompuSyn software and generated isobolograms according to the manufacturer's instructions (www.combosyn.com). The overall effects of drug combination were analyzed by the method of Chou and Talalay as described previously in detail.[15] Combination index <1.0 means synergism of the two drugs. The fraction affected (Fa) means the fraction of the population affected by drug treatment. (**c**) Non-obese diabetic/severe combined immunodeficient (NOD/SCID) mice aged 6 to 8 weeks were inoculated subcutaneously in the right thigh with 3×10^6 HBL-2 cells in 0.5 ml IMDM medium mixed with 0.5 ml Matrigel basement membrane matrix (Becton Dickinson, Franklin Lakes, NJ, USA).[14] When tumors were measurable (day 0), mice were assigned to four treatment groups: those receiving the vehicle alone (the control group), those receiving romidepsin alone, those receiving cyclophosphamide alone and those receiving cyclophosphamide plus romidepsin (the combination group) ($n = 3$–6 animals/group). Romidepsin was given intravenously through the tail vein at 0.1 mg/kg on days 0, 2, 5, 7 and 9.[14] Cyclophosphamide was given intraperitoneally at 50 mg/kg on days 2, 5, 7 and 9. The control group received the vehicle (0.9% NaCl) alone on the same schedule. (Left panel) Caliper measurements of the longest perpendicular tumor diameters were taken every alternate day to estimate the tumor volume using the following formula: $4/3\pi \times (\text{width}/2)^2 \times (\text{length}/2)$, which represents the three-dimensional volume of an ellipse. (Right panel) The *y* axis shows the average tumor volume of each group at day 0 and 14. The means ± s.d. (bars) are shown ($n = 3$–4). *P*-values were calculated by one-way ANOVA with Tukey's multiple comparison test. (**d**) We transfected the lentiviral short-hairpin RNA/small-interfering RNA (shRNA/siRNA) expression vector pLL3.7-HDAC3 shRNA or empty vector into 293FT cells with packaging plasmids (Invitrogen, Carlsbad, CA, USA) to produce infective lentiviruses in culture supernatants. Lentiviruses were added to HBL-2 cell suspensions in the presence of 8 μg/ml polybrene and transduced for 24 h. The transduced cells were washed with fresh medium and cultured for an additional 24 h, followed by collection of GFP-positive cells using a FACS Aria II flow cytometer (Becton Dickinson). shRNA-treated HBL-2 cells were resuspended in fresh medium and cultured with the indicated concentrations of bendamustine or 4-OHCY. Cell growth was determined by the MTT assay after 48 h. The *y* axis indicates the relative growth of drug-treated cells against untreated cells (Control) transduced with empty vector (Mock) or shHDAC3 vector. The means ± s.d. (bars) of three independent experiments are shown. *P*-values were calculated using one-way analysis of variance with the Student–Newman–Keuls multiple comparison test.

CONFLICT OF INTEREST

The authors declare no conflict of interest.

ACKNOWLEDGEMENTS

We thank Professor Martin JS Dyer (MRC Toxicology Unit, Leicester University, Leicester, UK) for providing NCEB-1 and Granta519 cell lines. This work was supported in part by the High-Tech Research Center Project for Private Universities: Matching Fund Subsidy from MEXT, a grant-in-aid for Scientific Research from JSPS (to YF and JK), and research grants from The Naito Foundation, The Yasuda Medical Foundation, The Uehara Memorial Foundation (to YF), Japan Leukemia Research Fund and Takeda Science Foundation (to JK). NH is a winner of the Young Scientist Award of Jichi Medical University.

N Hiraoka[1], J Kikuchi[1], D Koyama[1], T Wada[1], S Mori[2], Y Nakamura[3] and Y Furukawa[1]

[1]Division of Stem Cell Regulation, Center for Molecular Medicine, Jichi Medical University, Tochigi, Japan;
[2]Medical Education Center, Saitama Medical University, Saitama, Japan and
[3]Department of Hematology, Saitama Medical University, Saitama, Japan
E-mail: furuyu@jichi.ac.jp

REFERENCES

1 Horwitz GA, Zhang K, McBrian MA, Grunstein M, Kurdistani SK, Berk AJ. Adenovirus small e1a alters global patterns of histone modification. *Science* 2008; **321**: 1084–1085.
2 Eskandarian HA, Impens F, Nahori M-A, Soubigou G, Coppée J-Y, Cossart P *et al.* A role for SIRT2-dependent histone H3K18 deacetylation in bacterial infection. *Science* 2013; **341**: 1238858.
3 Barber MF, Michishita-Kioi E, Xi Y, Tasselli L, Kioi M, Moqtaderi Z *et al.* SIRT7 links H3K18 deacetylation to maintenance of oncogenic transformation. *Nature* 2012; **487**: 114–118.
4 Seligson DB, Horvath S, Shi T, Yu H, Tze S, Grunstein M *et al.* Global histone modification patterns predict risk of prostate cancer recurrence. *Nature* 2005; **435**: 1262–1266.
5 Manuyakorn A, Paulus R, Farrell J, Dawson NA, Tze S, Cheung-Lau G *et al.* Cellular histone modification patterns predict prognosis and treatment response in resectable pancreatic adenocarcinoma: results from RTOG 9704. *J Clin Oncol* 2010; **28**: 1358–1365.
6 Leshchenko VV, Kuo P-Y, Shaknovich R, Yang DT, Gellen T, Petrich A *et al.* Genomewide DNA methylation analysis reveals novel targets for drug development in mantle cell lymphoma. *Blood* 2010; **116**: 1025–1034.
7 Vose JM. Mantle cell lymphoma: 2012 update on diagnosis, risk-stratification, and clinical management. *Am J Hematol* 2012; **87**: 605–609.
8 Blackwell JS, Wilkinson ST, Mosammaparast N, Pemberton LF. Mutational analysis of H3 and H4 N termini reveals distinct roles in nuclear import. *J Biol Chem* 2007; **282**: 20142–20150.
9 Qian M-X, Pang Y, Liu CH, Haratake K, Du B-Y, Ji D-Y *et al.* Acetylation-mediated proteasomal degradation of core histones during DNA repair and spermatogenesis. *Cell* 2013; **153**: 1012–1024.
10 Bradner JE, West N, Grachan ML, Greenberg EF, Haggarty SJ, Warnow T *et al.* Chemical phylogenetics of histone deacetylases. *Nat Chem Biol* 2010; **6**: 238–243.
11 Summers AR, Fischer MA, Stengel KR, Zhao Y, Kaiser JF, Wells CE *et al.* Hdac3 is essential for DNA replication in hematopoietic progenitor cells. *J Clin Invest* 2013; **123**: 3112–3123.
12 Xia Y, Wang J, Liu T-J, Yung WKA, Hunter T, Lu Z. c-Jun downregulation by HDAC3-dependent transcriptional repression promotes osmotic stress-induced cell apoptosis. *Mol Cell* 2007; **25**: 219–232.
13 Escaffit F, Vaute O, Chevillard-Briet M, Segui B, Takami Y, Nakayama T *et al.* Cleavage and cytoplasmic relocalization of histone deacetylase 3 are important for apoptosis progression. *Mol Cell Biol* 2007; **27**: 554–567.
14 Shimizu R, Kikuchi J, Wada T, Ozawa K, Kano Y, Furukawa Y. HDAC inhibitors augment cytotoxic activity of rituximab by upregulating CD20 expression on lymphoma cells. *Leukemia* 2010; **24**: 1760–1768.
15 Kikuchi J, Yamada S, Koyama D, Wada T, Nobuyoshi M, Izumi T *et al.* The novel orally active proteasome inhibitor K-7174 exerts anti-myeloma activity *in vitro* and *in vivo* by down-regulating the expression of class I histone deacetylases. *J Biol Chem* 2013; **288**: 25593–25602.

Supplementary Information accompanies this paper on Blood Cancer Journal website (http://www.nature.com/bcj)